

A. CONTROLLED-POTENTIAL ELECTROMECHANICAL RESHAPING OF CARTILAGE

Reprinted with permission from Hunter, B. M.; Kallick, J.; Kissel, J.; Herzig, M.; Manuel, C.; Protsenko, D.; Wong, B. J. F.; Hill, M. G. Controlled-Potential Electromechanical Reshaping of Cartilage. *Angewandte Chemie* **2016**, *128*, 5587. DOI: 10.1002/ange.201600856. Copyright 2016 John Wiley and Sons.

A.1. Abstract

An alternative to conventional "cut-and-sew" cartilage surgery, electromechanical reshaping (EMR) is a molecular-based modality in which an array of needle electrodes is inserted into cartilage held under mechanical deformation by a jig. Brief (~2 min.) application of an electrochemical potential at the water-oxidation limit results in permanent reshaping of the specimen. Highly sulfated glycosaminoglycans within the cartilage matrix provide structural rigidity to the tissue via extensive ionic-bonding networks; this matrix is highly permselective for cations. Our studies indicate that EMR results from electrochemical generation of localized, low-pH gradients within the tissue: fixed negative charges in the proteoglycan matrix are protonated, resulting in chemically induced stress relaxation of the tissue. Re-equilibration to physiological pH restores the fixed negative charges, and yields remodeled cartilage that retains a new shape approximated by the geometry of the reshaping jig.

A.2. Introduction

Hyaline cartilage forms underlying structural features of the head and neck, and serves a critical functional role in the upper airway.¹ Congenital defects, trauma, and disease can damage cartilage tissue, necessitating surgical intervention to reshape (or replace) damaged (or missing) structures.² Conventional open surgery is characterized by long recovery times, significant tissue morbidity, and high cost; reshaping living tissue using less invasive

techniques is thus the subject of active research.^{3,4} Most alternative methods focus on modifying the bulk mechanical properties of cartilage—*i.e.*, using laser- or RF-heat generation to denature and/or accelerate stress relaxation—by exploiting the thermoviscoelasticity common to collagenous tissues.⁵ Our work instead focuses on novel electrochemical modalities that transiently alter the chemical properties of tissue, providing a molecular-based alternative to the scalpel and sutures.

Originally conceived as a thermal technique in which electrical current flow through cartilage would cause resistive heating,⁶ “electromechanical reshaping” (EMR) was developed as a low-cost technique for reshaping cartilage. EMR combines mechanical deformation with the application of electric fields: in a typical embodiment, cartilage is held in mechanical deformation by a mold, needle electrodes are inserted into the tissue, and a constant voltage (*e.g.*, 5 V) is applied across the specimen for several minutes. When the electrodes and mold are removed, the cartilage assumes a new shape that approximates the geometry of the mold (*e.g.*, a 90° bend).⁷

Although effective shape change has been demonstrated in several animal models,^{8,9} the process often is accompanied by tissue injury near the electrode-insertion sites; moreover, the relationship between shape change and the duration and magnitude of the applied voltage can be unpredictable. The lack of detailed mechanistic insight into the molecular changes that occur during EMR has impeded its development as a practical clinical tool. Indeed, careful measurements recorded during EMR reveal negligible tissue heating ($< 2^{\circ}\text{C}$),¹⁰ indicating a mechanism of action quite distinct from conventional thermoforming. Here, we report the results of simple electrochemical assays that indicate EMR-induced tissue remodeling is a chemical process that depends on the generation of highly localized pH gradients within cartilage under mechanical stress. Carefully controlling the electrolysis conditions has enabled us to reshape *ex vivo* tissue both predictably and reproducibly, with minimal cell mortality. These results position EMR as a potentially transformative, ultra-low-cost, chemical-based surgical therapy, suitable for point-of-care implementation.

A.3. Cartilage Structure and Permselectivity

Cartilage tissue is a polymer hydrogel (~75% water by weight) consisting of highly organized collagen fibrils surrounded by a proteoglycan matrix.¹¹ Highly sulfated and carboxylated glycosaminoglycans (GAGs) that are deprotonated under physiological conditions provide a substantial fixed negative charge to the tissue, resulting in an ionic-bond network that provides structural rigidity. Chondrocytes are sparsely populated within this extracellular matrix, governing homeostasis and repair processes; maintaining chondrocyte viability is particularly important, as inflammation following trauma can lead to unregulated production of fibrocartiliginous tissue, with subsequent susceptibility to scarring and loss of function.¹²

Given the analogous structural elements common both to cartilage and synthetic polyelectrolytes (*e.g.*, Nafion), we suspected that cartilage tissues might exhibit strong permselectivity to cations.¹³ We thus prepared thin (~100 μm) sections of costal cartilage¹⁴ to serve as membranes between two concentration cells that contained different activities of sodium chloride. For a material that is ideally permselective, the membrane (Donnan) potential between two reference electrodes placed separately into these cells is given by:

$$E_{mem} = \frac{RT}{F} \ln\left(\frac{a_1}{a_2}\right),$$

where a_1 and a_2 are the respective activities of Na^+ in the two chambers. At 25°C, a plot of E_{mem} vs. $\log(a_1/a_2)$ should yield a straight line with slope equal to 59 mV per decade. As illustrated in Figure A.1, voltage measurements obtained across a cartilage membrane result in a slope (44 ± 6 mV/decade)¹⁵ that is remarkably close to that found in analogous experiments where Nafion is used instead;¹⁶ as with the synthetic polyelectrolyte, the slightly lower-than-ideal slope suggests that some sodium ions are able to migrate through the tissue, likely as ion-pairs.

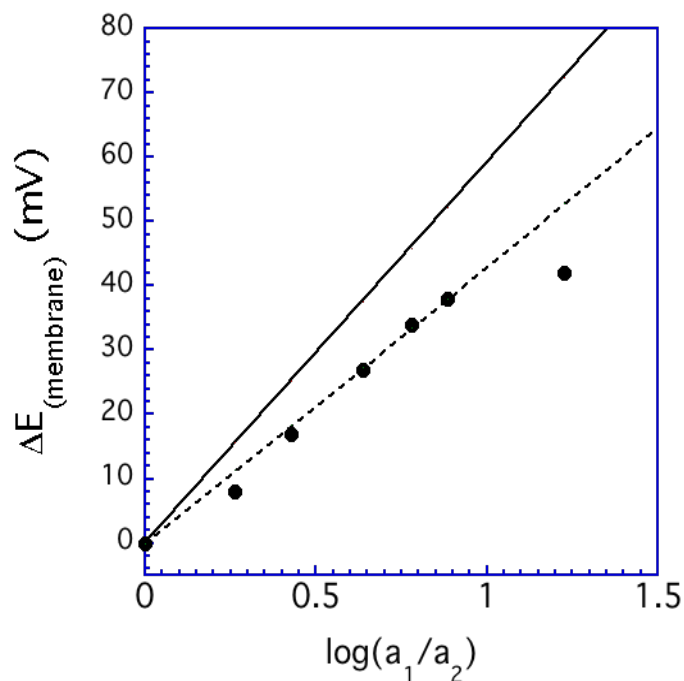


Figure A.1. Plot of potential difference (ΔE_{mem}) measured between two concentration cells featuring identical AgCl/Ag reference electrodes, separated by a ~ 100 μm thick cartilage membrane. Solid line corresponds to ideal permselective response (59 mV/decade). The activity of Na^+ in chamber two was fixed at 0.0059 M. All solutions contained 5 mM sodium phosphate, adjusted to pH 7.4 with HCl.

Notably, the slope of the cartilage-membrane potential should begin to flatten out when the concentration of NaCl in one of the chambers approaches the fixed-charge density (FCD) within the tissue: at this point Donnan exclusion of anions is less complete and the membrane potential levels off. In our system, this flattening occurs at a salt concentration of ~ 0.15 M—a value fully consistent with the FCD of articular cartilage measured *via* MRI,^{17,18} computed tomography (CT),^{19,20} and fluorescence-labeling²¹ methods. Evaluating the permselectivity response of cartilage membranes, therefore, provides an alternative for quantifying the FCD of tissue samples.

A.4. Molecular mechanism of EMR

We considered several modes of action for electromechanical tissue reconstruction: (i) dehydration of the hydrogel matrix followed by tissue denaturation; (ii) electrophoresis; and (iii) chemical modification of the GAG matrix. To distinguish between these possibilities, we carried out a series of electrolysis experiments using a biopotentiostat that featured two working-electrode arrays. Figure A.2 shows the cyclic voltammogram recorded at a platinum electrode inserted into rabbit septal cartilage immersed in phosphate-buffered saline (PBS), pH 7.4. The respective cathodic and anodic currents correspond to the solvent limits for hydrogen evolution and water oxidation recorded under identical conditions in the absence of cartilage. Notably, oxidation of chloride to chlorine (with subsequent conversion to hypochlorite) is also expected at the positive potential.

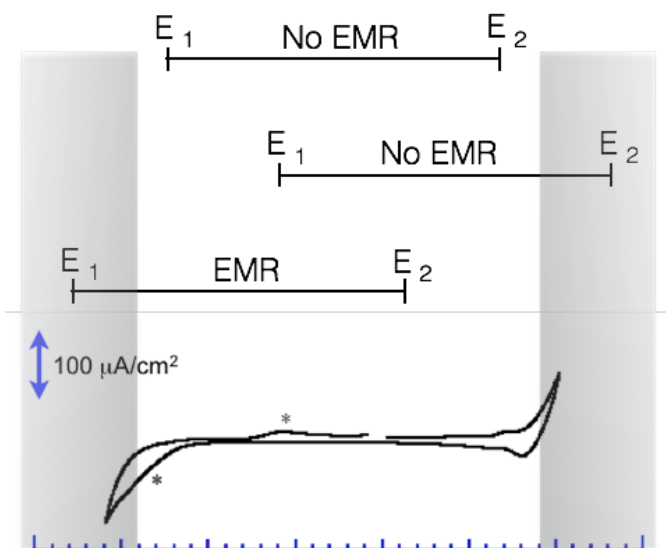


Figure A.2. Cyclic voltammogram recorded at a platinum electrode inserted into a ~ 2 -mm thick section of rabbit septal cartilage submerged in PBS buffer. (Scan rate = 50 mV/sec; the response due to chloride oxidation and re-reduction is indicated by *.) Shaded areas mark respective potential thresholds for water oxidation (onset ~ 1.4 V *vs.* AgCl/Ag) and reduction (onset ~ -0.9 V *vs.* AgCl/Ag). Horizontal lines represent applied-potential gradients (E_1 and E_2 for EMR trials).

Using a 90°-reshaping jig²² (Figure A.3), we next performed a series of reshaping experiments. To decouple the effects of voltage gradients, current flow, and applied potentials on the shape-changing process, the two sets of working electrodes were held at a constant potential difference (2 V), while the midpoint of those potentials was scanned between ± 1 V (*vs.* AgCl/Ag). Because the bipotentiostat directs electron flow between the working electrodes and a remote auxiliary electrode, current does not pass directly through the tissue.

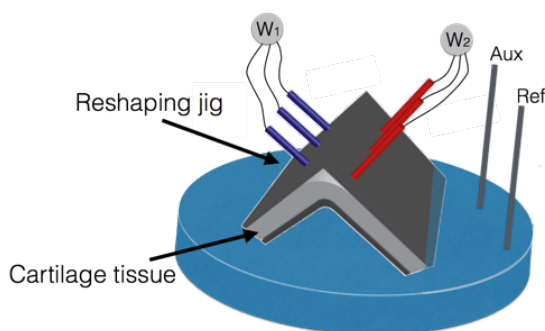


Figure A.3. Illustration of the EMR apparatus. W_1 and W_2 correspond to the two arrays of platinum-needle working electrodes.

Significantly, EMR occurs *only* when the potential of at least one set of working electrodes is held positive of the anodic limit. No potential gradient across the tissue is required; indeed, reshaping is measurably more effective when both sets of working electrodes are held positive of the water-oxidation threshold.

As illustrated in Figure A.4.A, the cartilage bend angle, θ , plotted for multiple trials *vs.* the applied potential during EMR reveals reshaping efficiencies that vary widely from run to run (albeit with a trend toward greater shape change (smaller θ) at higher potentials). However, re-plotting θ *vs.* the charge passed during each experiment (Figure A.4.B) shows

that the magnitude of EMR correlates directly with the total charge transferred, regardless of the applied potential.

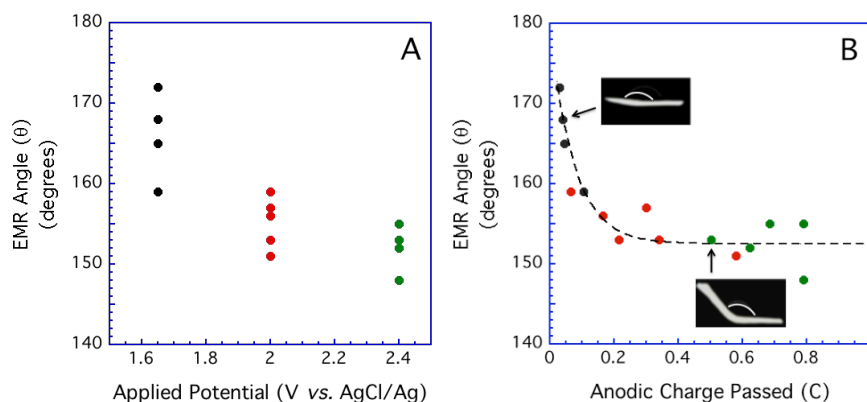


Figure A.4. (A) EMR “bend angle”, θ , for multiple samples of rabbit-septal cartilage following a 2-minute electrolysis at 1.65 V (black), 2.0 V (red), and 2.4 V (green) *vs.* AgCl/Ag. Note the range of bend angles at each applied potential. (B) The same θ data re-plotted *vs.* the anodic charge passed during each run. Insets: images of reshaped cartilage following 0.05 C and 0.5 C passed.

We propose that acidification at the anode (a consequence of water oxidation) and subsequent diffusion of protons into the tissue is the dominant process responsible for shape change. Protonation of immobilized anions within the GAG matrix disrupts the ionic-bonding network that provides structural integrity to the tissue. This, in turn, relieves the stress imposed by mechanical deformation. Re-equilibration to physiological pH restores the FCD after molecules have locally “shifted” and reestablishes the ionic-bonding matrix, resulting in sustained shape change of the tissue. It is noteworthy that this mechanism explains our observation that EMR persists *ex vivo* only if the pH is re-equilibrated in neutral buffer for several minutes following electrolysis; if the specimen is instead removed from the jig immediately after electrolysis, the tissue is noticeably more malleable near the electrode placements.

This mechanism also explains why the maximum EMR-bend angles in Figure A.4 are significantly larger than (the ideal) 90° . Bending the tissue induces both tensile and compressive stress localized within the matrix;²³ chemically induced stress relaxation occurs only when the fixed negative charges at those loci lie within the diffusion radius of protons generated *via* electrolysis (~ 1 mm). It is evident from the plots of θ vs. charge that under these experimental conditions the maximum shape change is reached by ~ 0.5 C passed. That charge is sufficient to generate a pH gradient low enough to fully neutralize the FCD proximal to the individual electrodes in the array: stressed tissue outside of the diffusion radius remains unaffected by the EMR process and is therefore not remodeled. Indeed, placing electrodes above *and* below the axis of inertia of bent tissues results in more effective cartilage remodeling, as both tension and compression are chemically relaxed.

A.5. pH Dependence of Shape Change

Given this model, the pH threshold for inducing shape change should correspond to the pK_a of the sulfonic and carboxylic acid functional groups of the GAGs.²⁴ It follows that neutralizing the FCD would cause a loss of permselectivity, and that loss would be reflected in smaller Donnan potentials across the cartilage membrane. This is precisely what we find. Figure 4A shows several plots of E_{mem} vs. $\log(a_1/a_2)$ recorded as a function of pH. The slopes depend strongly on the pH of the solution, approaching zero at $\sim \text{pH } 1$. Plotting the slopes vs. the solution pH produces a sigmoidal response (Figure 4B), from which we calculate an effective tissue pK_a of ~ 3.5 .

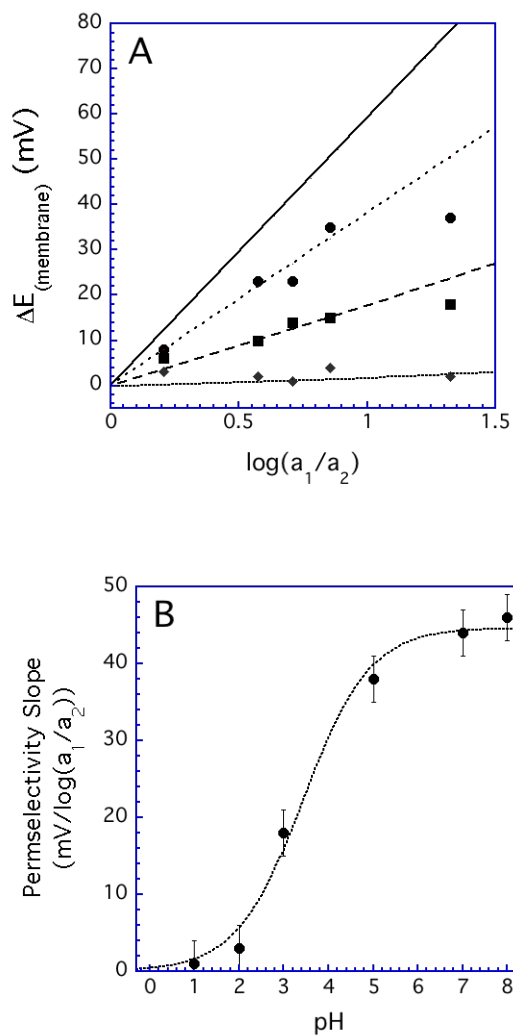


Figure A.5. (A) Plot of E_{mem} between two AgCl/Ag reference electrodes placed into concentration cells separated by a ~ 100 μm cartilage membrane, recorded at different pH values. (●) pH 5; (■) pH 3; (▲) pH 1. Tissues were equilibrated at the given pH for 5 minutes before data collection. Solid line corresponds to an ideal permselective response. (B) Plot of the “Permeability Slope” as a function of solution pH.

A.6. Conclusions

In contrast to conventional surgical procedures that rely on carving, cutting, suturing, or morselizing cartilage to produce physically altered structures, EMR exploits chemical reactions (water oxidation/proton diffusion) that are both highly localized *and* highly

reversible to remodel tissue. By restoring physiological pH following EMR, remodeled cartilage regains its FCD and exhibits physical properties indistinguishable from untreated tissues.²⁶ Combined with previously developed finite-element models that map the internal stress within mechanically deformed tissues, coulometric analysis can be used to “dose” the EMR process to ensure maximal shape change while avoiding over-oxidation (and over-acidification). These experiments thus provide a roadmap for developing EMR as a chemical-based surgical therapy that operates by reversibly altering the inherent physical properties of tissue at the molecular level.

A.7. Experimental Section

Electrochemical measurements were carried out using a Princeton Applied Research VersaSTAT 4/3F bipotentiostat/galvanostat. Potentials are reported vs. AgCl/Ag in 1M KCl.

Polycarbonate concentration cells (~20 mL) featured matching 1-cm diameter holes surrounded by o-ring fittings. Cartilage membranes were positioned between the two o-rings, and the cells were clamped together prior to permselectivity assays. Donnan potentials were measured by recording the potential difference between two AgCl/Ag reference electrodes placed into each cell, using a Keithley Model 2000 digital voltmeter. 100-um thick cartilage membranes were cut from fresh porcine costal cartilage.

EMR experiments were carried out using a needle-based reshaping jig. Rabbit septal cartilage was harvested from specimens obtained from a local abattoir. Samples were loaded into the reshaping jig and partially submerged in PBS prior to electrolysis. The jig was then transferred into a large beaker containing fresh PBS and soaked for five minutes. The specimen was removed from the jig, digitally photographed, and the reshaping angle was measured using commercial software (Screen Protractor, Iconico).

Chondrocyte viability was monitored using a “live/dead” assay as previously described.²⁶ Specimens subjected to potential-controlled EMR exhibited only minimal chondrocyte mortality compared to untreated samples.

A.8. References and Notes

- [1] Hanson, J.T. *Netter's Clinical Anatomy, Third Edition*; Elsevier Saunders: Philadelphia, PA, 2014.
- [2] Lorenz, R.R. *Curr. Op. in Otolaryngology & Head & Neck Surgery* **2003**, *11*, 467.
- [3] V. Oswal, M. Remacle, *Lasers in Otorhinolaryngology and Head and Neck Surgery, 2nd Ed.*, Kugler Publications: Amsterdam, 2014.
- [4] Wormald, J.C.R.; Fishman, J.M.; Juniati, S.; Tolley, N.; Birchall, M.A. *J. Laryngol. Oto.* **2015**, *129*, 732.
- [5] Baek, S.; Wells, P.B.; Rajagopal, K.R.; Humphrey, J.D. *J. Biomech. Eng.* **2005**, *127*, 580.
- [6] Protsenko, D.E.; Ho, K.; Wong, B.J.F. *Annals Biomed. Eng.* **2006**, *34*, 455.
- [7] Manuel, C.T.; Foulad, A.; Protsenko, D.E.; Sepehr, A.; Wong, B.J.F. *Ann. Biomed. Eng.* **2010**, *38*, 3389.
- [8] Hussain, S.; Manuel, C.T.; Protsenko, D.E.; Wong, B.J.F. *Laryngoscope* **2015**, *125*, 1628.
- [9] Animal models show that memory effects result in some shape recidivism (both acute and longer-term) of cartilage treated by EMR. Clinical procedures would likely require “over correction” to achieve the desired long-term shape. See, for example: Badran, K.W.; Manuel, C.T.; Loy, A.C.; Conderman, C.; Yau, Y.Y; Lin, J.; Tjoa, T.; Su, E.; Protsenko, D.; Wong, B.J.F. *Laryngoscope* **2015**, *125*, 2058.
- [10] Ho, K.H.K.; Valdes, S.H.D.; Protsenko, D.E.; Aguliar, G.; Wong, B.J.F. *Laryngoscope* **2003**, *113*, 1916.

- [11] Poole, A.R.; Kojima, T.; Yasuda, T.; Mwale, F.; Kobayashi, M.; Leverty, S. *Curr. Ortho. Prac.* **2001**, *391*, S26.
- [12] Loeser, R.F. *Arthritis Rheum.* **2006**, *54*, 1357.
- [13] Naegeli, R.; Redepenning, J.; Anson, F.C. *J. Phys. Chem.* **1986**, *90*, 6227.
- [14] Foulard, A.; Manuel, C.; Wong, B.J.F. *Arch. Facial Plast. Surg.* **2011**, *13*, 259.
- [15] Error in the permselectivity response (i.e., the slope of ΔE_{mem} vs. $\log(a_1/a_2)$) for any given run was typically quite small, cf., Figure A.1. There was, however, considerable sample-to-sample variability: at pH 7.4 individual slopes ranged from $\sim 40 - 50$ mV/decade depending on the individual specimen.
- [16] Redepenning, J.; Anson, F.C. *J. Phys. Chem.* **1989**, *91*, 4549.
- [17] Kneeland, J.B.; Reddy, R. 2007, *J. Magn. Reson. Im.* **2007**, *25*, 339.
- [18] Freedman, J.D.; Lusic, H.; Wiewiorski, M.; Farley, M.; Snyder, B.D.; Grinstaff, M.W. *Chem. Commun.* **2015**, *51*, 11166.
- [19] Bansal, P.N.; Joshi, N.S.; Entezari, V.; Malone, B.C.; Stewart, R.C.; Snyder, B.D.; Grinstaff, M.W. *J. Ortho. Res.* **2011**, *29*, 704.
- [20] Freedman, J.D.; Lusic, H.; Snyder, B.D.; Grinstaff, M.W. *Angew. Chem. Int. Ed.* **2014**, *53*, 8406.
- [21] Hyun, H.; Owens, E.A.; Wada, H.; Levitz, A.; Park, G.; Park, M.H.; Frangioni, J.V.; Henary, M.; Choi, H.S. *Angew. Chem. Int. Ed.* **2015**, *54*, 8648.
- [22] Wu, E.C.; Protsenko, D.E.; Khan, A.Z.; Dubin, S.; Karimi, K.; Wong, B.J.F. *IEEE T. Bio-Med. Eng.* **2011**, *58*, 2378.

[23] Protsenko, D.E.; Wong, B.J.F. *Laser. Surg. Med.* **2007**, *39*, 245.

[24] Du, Y.; Taga, A.; Suzuki, S.; Liu, W.; Honda, S. *J. Chromatogr. A* **2002**, *947*, 287.

[25] This value is slightly higher than analogous solution pK_a's of the GAG functional groups (~2.5 – 3),²⁴ suggesting a more hydrophobic environment inside of the tissue that renders the groups slightly less acidic.

[26] Protsenko, D.E.; Ho, K.; Wong, B.J.F. *Ann. Biomed. Eng.* **2011**, *39*, 66.